J. Membrane Biol. 147, 121–136 (1995)

The Journal of
Membrane
Biology

Characterization of a Chloride Channel Reconstituted from Cardiac Sarcoplasmic Reticulum

C. Townsend,[1] R.L. Rosenberg[1,2]

[1]Department of Pharmacology, University of North Carolina, Chapel Hill, NC 27599-7365
[2]Departments of Pharmacology and Physiology, University of North Carolina, Chapel Hill, NC 27599-7365

Received: 6 March 1995/Revised: 5 May 1995

Abstract. We have characterized a voltage-sensitive chloride channel from cardiac sarcoplasmic reticulum (SR) following reconstitution of porcine heart SR into planar lipid bilayers. In 250 mM KCl, the channel had a main conductance level of 130 pS and exhibited two substrates of 61 and 154 pS. The channel was very selective for Cl^- over K^+ or Na^+ (P_{K^+}/P_{Cl^-} = 0.012 and P_{Na^+}/P_{Cl^-} ~ 0.040). It was permeable to several anions and displayed the following sequence of anion permeability: $SCN^- > I^- > NO_3^- \sim Br^- > Cl^- > F^- > HCOO^-$. Single-channel conductance saturated with increasing Cl^- concentrations (K_m = 900 mM and γ_{max} = 488 pS). Channel activity was voltage dependent, with an open probability ranging from ~1.0 around 0 mV to ~0.5 at +80 mV. From −20 to +80 mV, channel gating was time-independent. However, at voltages below −40 mV the channel entered a long-lasting closed state. Mean open times varied with voltage, from ~340 msec at −20 mV to ~6 msec at +80 mV, whereas closed times were unaffected. The channel was not Ca^{2+}-dependent. Channel activity was blocked by disulfonic stilbenes, arylaminobenzoates, zinc, and cadmium. Single-channel conductance was sensitive to *trans* pH, ranging from ~190 pS at pH 5.5 to ~60 pS at pH 9.0. These characteristics are different from those previously described for Cl^- channels from skeletal or cardiac muscle SR.

Key words: Chloride channel — Cardiac sarcoplasmic reticulum — Planar lipid bilayer — Ion selectivity — Voltage — Block — pH

Introduction

In heart, as in skeletal muscle, contraction is triggered by a rapid increase in intracellular free calcium concentration. This transient rise in calcium is initiated by a depolarization of the surface membrane which leads to calcium release from the sarcoplasmic reticulum (SR), during the excitation-contraction (E-C) coupling process. In heart muscle, SR Ca^{2+} release depends on the influx of extracellular calcium through L-type calcium channels (Fabiato, 1983). In contrast, skeletal muscle E-C coupling is independent of extracellular calcium, and is thought to occur by a mechanical coupling mechanism involving a direct interaction between L-type calcium channels and calcium-release channels located in the SR (Ríos & Pizarro, 1991). In both types of muscle, released calcium then activates the contractile proteins of the myofibrils. Muscle relaxation occurs when calcium is pumped back into SR through a Mg^{2+}-dependent Ca^{2+} ATPase.

In addition to being permeable to calcium, the SR membrane also allows the movement of small monovalent ions, including K^+, Na^+, H^+, and Cl^- (Miller, 1978; Meissner & McKinley, 1982; Meissner, 1983). Although a physiological role for these permeation pathways is not clear, it has been proposed that they permit rapid ionic movements across the SR membrane to counter electrogenic calcium fluxes during calcium release and uptake (Meissner, 1983; Garcia & Miller, 1984). Miller (1978) first reported the observation of single K^+ and Cl^- channels from SR after incorporation of SR vesicles into planar lipid bilayers.

Since this first report, several SR Cl^- channels from skeletal and cardiac muscle have been identified after reconstitution of SR into bilayers or in direct patch clamp studies. Tanifuji, Sokabe, and Kasai (1987) reported a skeletal SR Cl^- channel with a conductance of 200 pS in 100 mM Cl^-. Rousseau, Roberson, and Meissner (1988) reported a smaller Cl^- channel, 95 pS in 260 mM Cl^-, from skeletal muscle. Palade and coworkers used a direct patch clamp technique to study SR channels and observed large, voltage-sensitive Cl^- channels (505 pS in

Correspondence to: R.L. Rosenberg

Table 1. Membrane marker analysis

Membrane preparation	SERCA-2 immunoreactivity (% maximum)	Ryanodine binding (pmol/mg)	Na^+/K^+ ATPase activity (μmol/mg/min)	Cl^- channel incorporation (% of experiments)
Sarcolemma	51.08	0.177	3.237	29.0
SR I	100.00	2.044	0.215	52.5
SR II	48.11	0.822	0.027	22.0

Values for SERCA-2 immunoreactivity, ryanodine binding, and Na^+/K^+ ATPase assays are from one membrane preparation. Values for channel incorporation are from 3 preparations. SR I, light sarcoplasmic reticulum fraction; SR II, heavy sarcoplasmic reticulum fraction.

200 mM Cl^-) from skeletal muscle SR (Hals, Stein, & Palade, 1989). Rousseau (1989) reported the observation of Cl^- channels from cardiac SR. These channels have a conductance of 55 pS in 260 mM Cl^- and are sensitive to membrane voltage. Larralde and Nasi (1989) described the properties of a 140 pS Cl^- channel (in 200 mM Cl^-) from toad skeletal muscle SR. In addition, Ide et al. (1991) described the purification and reconstitution of a 115 pS Cl^- channel (in 300 mM Cl^-) in SR membranes from rabbit skeletal muscle. More recently, Kawano and coworkers published the results of bilayer studies on a 116 pS Cl^- channel (in 500 mM Cl^-) from cardiac SR (Kawano et al., 1992; Kawano & Hiraoka, 1993). This channel is voltage-insensitive and is regulated by protein kinase A and Ca^{2+}-calmodulin.

We now report the observation of a Cl^- channel from cardiac SR with characteristics different from those of previously described SR anion channels. The goal of the present study was to describe the biophysical and pharmacological properties of this channel after incorporation of cardiac sarcoplasmic reticulum membranes into planar lipid bilayers. We determined its conductance in various Cl^- concentrations, examined its ionic selectivity, voltage dependence, and sensitivity to pH and various Cl^- channel blockers. A preliminary report of some of this work has been presented in abstract form (Townsend & Rosenberg, 1994).

Materials and Methods

Chemicals and Solutions

1-Palmitoyl-2-oleoyl-phosphatidylethanolamine and 1-palmitoyl-2-oleoyl-phosphatidylserine were from Avanti Polar Lipids (Alabaster, AL). Leupeptin, pepstatin A, PMSF (phenyl methyl sulfonyl fluoride), and aprotinin were from United States Biochemical (Cleveland, OH). DNDS (dinitrostilbene disulfonic acid) was from Pfalz and Bauer (Waterbury, CT). NPPB was kindly provided by Dr. R. Greger (Freiburg, FRG). Stocks solutions of DNDS and NPPB were prepared in dimethylsulfoxide. All other chemical were from Sigma Chemical (St. Louis, MO).

Preparation of Cardiac Sarcoplasmic Reticulum Membranes

Cardiac SR membranes were prepared from pig left ventricle as described (Anderson et al., 1989; Darling, Lai, & Meissner, 1992). A pig was anesthetized, and following a median sternotomy, the heart was rapidly excised and placed in ice-cold 0.3 M sucrose. All following steps were done at 4°C. The entire ventricle (~100 g) was trimmed of large fatty deposits, minced, and homogenized in 10 volumes of (in mM) 0.3 sucrose, 0.5 EDTA, 20 Tris-Hepes, pH 7.4, containing a mixture of protease inhibitors (100 nM aprotinin, 2 μM leupeptin, 1 μM pepstatin A, 1 mM benzamidine, 1 mM iodoacetamide, and 0.2 mM PMSF) in a Waring blender (2 bursts of 30 sec). The homogenate was centrifuged for 20 min at 5,000 rpm in a GSA rotor (3,600 × g_{max}). The resulting supernatant was filtered through two layers of cheesecloth and centrifuged for 60 min at 33,000 rpm in a Beckman 45 Ti rotor (122,000 × g_{max}). After resuspension of the pellets in 60 ml of 0.6 M KCl, 0.1 mM $MgCl_2$, 0.1 mM EGTA, 50 μM $CaCl_2$, 10 mM K-Pipes, pH 7.0 containing 1 μM leupeptin and 0.2 mM PMSF, membranes were placed at the top of a discontinuous sucrose gradient (20, 30, and 40% w/w sucrose in the 0.6 M KCl buffer described above) and centrifuged overnight at 26,000 rpm in a SW28 rotor (126,000 × g_{max}). Membranes at the 20–30% and 30–40% sucrose interfaces (light and heavy SR, respectively) were collected, diluted with 2 volumes of deionized water, and sedimented by centrifugation for 45 min at 33,000 rpm in a Beckman 45 Ti rotor (120,000 × g_{max}). The resulting pellets were resuspended in 0.3 M sucrose, 10 mM K-Pipes, pH 7.0, frozen in liquid nitrogen, and stored at −80°C for up to 6 months.

Preparation of Cardiac Sarcolemmal Membranes

Porcine hearts were obtained from animals killed at a local slaughterhouse. Membranes were prepared from left ventricular muscle by homogenization, differential centrifugation and a one-step sucrose density gradient fractionation as described (Rosenberg, Hess, & Tsien, 1988). These membranes were frozen in liquid nitrogen and kept at −80°C for up to 6 months.

Membrane Marker Analysis and Channel Localization

Cl^- channels were reconstituted from the two membrane preparations described above. In our initial experiments, the sarcolemmal membrane preparation was used. Because Cl^- channels were readily incorporated into bilayers from these membranes, we initially thought that they were located at the cell surface (Townsend & Rosenberg, 1994). However, although our sarcolemmal membrane preparation was highly enriched in surface membrane markers (e.g., ~80-fold enrichment in Na^+/K^+ ATPase activity over crude homogenate), membrane marker analysis showed that it did contain some SR membranes (Table 1). SERCA-2, the Ca^{2+}-ATPase that is localized in the cardiac SR, and ryanodine receptor (the Ca^{2+}-release channel of the SR) were used as markers for SR membranes, and ouabain-sensitive Na^+/K^+ ATPase was used as a cell surface marker. SERCA-2 immunoreactivity was assessed by immunoblot analysis with monoclonal antibodies to

SERCA-2 as described (Jorgensen et al., 1988; Waldo et al., 1991). To quantify the immunoreactivity, Western blots were first scanned with a ScanMaker IIXF scanner (Microtek) and the scanned blots were then analyzed with ImageQuant (Molecular Dynamics). Ryanodine binding activity was determined as described (Darling et al., 1992) except that the binding reaction was done at 10°C for ~15 hr. Ouabain-sensitive Na^+/K^+ ATPase activity was determined as described by Forbush (1983). Protein concentrations were assayed with a BCA protein assay (Pierce, Rockford, IL).

The results from Table 1 show that the sarcolemma preparation contains a substantial amount of SR membranes, as SERCA-2 immunoreactivity was fairly abundant and some ryanodine binding sites were detected. Also, fusion of membrane vesicles from the sarcolemma preparation occasionally resulted in the incorporation of SR K^+ channels. In addition, Cl^- channels were observed after fusion of heavy SR membranes which are virtually devoid of surface membrane, as the Na^+/K^+ ATPase activity for this membrane fraction is very low. Taken together, these observations suggest that the channels are located in the SR.

Planar Lipid Bilayers Recordings

Bilayers composed of a mixture of 20 mg/ml lipids in decane (15 mg/ml 1-palmitoyl-2-oleoyl-phosphatidylethanolamine, and 5 mg/ml 1-palmitoyl-2-oleoyl-phosphatidylserine) were formed over a 100 μm hole in a polyvinyldifluoride partition. Bilayer formation was monitored by eye. At the time of bilayer formation, the aqueous solution on both sides of the membrane contained 50 mM saline (e.g., KCl), 10 mM HEPES, pH 7.0. After the bilayer formed, 200 mM saline and vesicles (light SR, heavy SR, or sarcolemma, 20–40 μg protein/ml) were added to the *cis* chamber. The presence of an osmotic gradient across the bilayer was necessary for channel incorporation, but no additional calcium was required. In order to facilitate fusion, the bilayer was then broken and immediately reformed. Channel incorporation usually occurred within the next 5 min. If needed, addition of ions, drugs, or other molecules was done by adding an aliquot of a stock solution to the *cis* or *trans* compartment.

Data Acquisition

Data acquisition was as previously described (Rosenberg & Chen, 1991) with an 80486-based computer running AxoBasic (Axon Instruments, Foster City, CA). The voltage was defined as *cis* relative to *trans* (cytoplasmic relative to lumenal, assuming standard fusion of outside-out SR vesicles). Currents flowing from *cis* to *trans* (i.e., Cl^- flowing from *trans* to *cis*) are shown as upward transitions. Unless otherwise specified, currents were filtered at 200 Hz (−3 dB, 8-pole Bessel lowpass), digitized at 1 kHz, and stored in computer memory for later analysis.

For open- and closed-times analysis, single-channel currents were recorded on videotape, and later filtered and digitized. To minimize the detection of false events, the filter frequency was chosen as a function of the standard deviation (σ_n) determined from the Gaussian distribution of the filtered baseline noise, so that σ_n was 10–20% of the single-channel amplitude (Colquhoun & Sigworth, 1983). The filtered data were then digitized at 25 times the −3 dB frequency (Magleby, 1992).

Data Analysis

Data were analyzed with an in-house AxoBasic analysis program. Unitary current amplitudes were determined by eye with computer-drawn lines that fit the closed and open channel levels. Open probability was calculated on a sweep-by-sweep basis by integrating the current for each sweep and normalizing it to that value expected for a channel open for 100% of the time. Open- and closed-times were determined automatically with a threshold set at 50% of the single-channel current. Recordings with transitions to the 60 pS substate (~50% of the main conductance level) were excluded from this analysis.

Interval histograms were constructed in an analysis program written in VisualBasic by Dr. Barry Pallotta (UNC, Pharmacology). In this program, open and shut durations are plotted on a logarithmically-binned time scale, and the square-roots of the number of events are plotted on the y-axis (Sigworth & Sine, 1987). This representation is useful for the display of rates that differ from several orders of magnitude. This program first corrects for sampling promotion error (Korn & Horn, 1988). The histograms are then fitted by the sum of exponentials that have the maximum likelihood of describing the data (Sigworth & Sine, 1987; McManus & Magleby, 1988).

For analysis of fast block, blocking and unblocking rate constants were derived from amplitude distributions as described by Yellen (1984). In this analysis, amplitude histograms of filtered current records are fit to the normalized beta distribution.

$$f(y) = y^{a-1}\,(1 - y)^{b-1} \tag{1}$$

with

$$a = \alpha\tau \tag{2}$$

and

$$b = \beta\tau \tag{3}$$

where y is the range of normalized amplitudes between 0 (blocked) and 1 (unblocked), α and β are the unblocking and blocking rate constants, respectively, and τ is the effective time constant of the filter (equal to $0.228/f_c$, where f_c is the −3 dB cutoff frequency of the low-pass filter). This analysis assumes that block arises from a filtered, two-state (blocking-unblocking) process where the single channel current level of the blocked state is 0 pA and the current level of the unblocked state is the same as the open state. Equilibrium dissociation constants (K_{Ds}) were determined from the equation:

$$K_D = (\alpha/\beta)\ [\text{blocker}] \tag{4}$$

Amplitude histograms were constructed from partially blocked open channel events (200 Hz filter frequency, 1 kHz sample rate), normalized to the fully open amplitude previously determined for the unblocked channel, and fit by eye with Eq. 1 convolved with the Gaussian distribution that describes the closed channel noise.

Results

Single Cl^- Selective Channels from Cardiac Sarcoplasmic Reticulum

Cl^- selective channels were observed following the incorporation of cardiac sarcoplasmic reticulum membranes into planar lipid bilayers. Figure 1*A* shows recordings from one of these channels at various membrane voltages in the presence of 350 mM KCl *cis* and 150 mM KCl *trans*. Under these conditions, the reversal

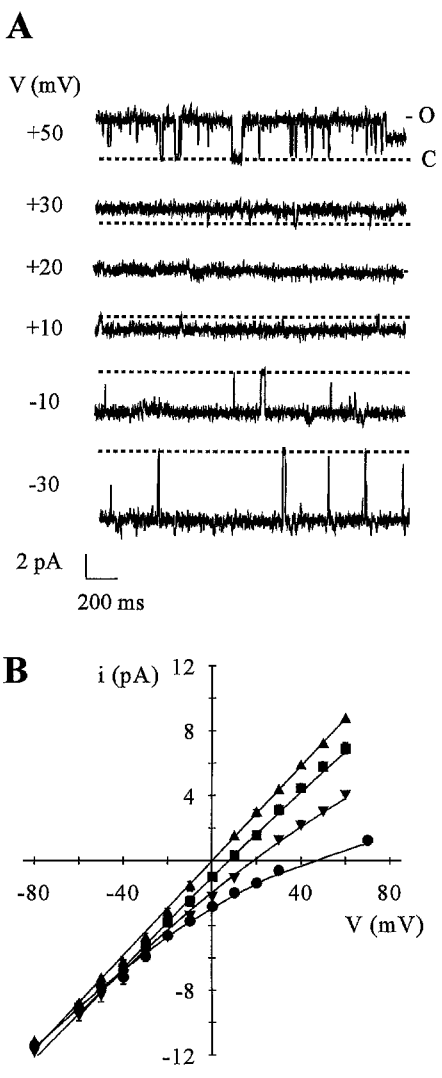

Fig. 1. (*A*) Example of recordings of reconstituted Cl^- channels. Single-channel currents were recorded in 350 mM KCl *cis* and 150 mM KCl *trans*. Membrane voltages are indicated on the left. The dotted lines represent the closed levels. (*B*) Single-channel current-voltage relations in various *trans* Cl^- concentrations. *Trans* Cl^- was changed from 50 mM (●) to 150 (▼), 250 (■), and 350 mM (▲); *cis* Cl^- was 350 mM. Data points are means ± SD from 3 experiments.

potential was very close to the equilibrium potential for Cl^- (E_{rev} ~ +20 mV and E_{Cl^-} = +19 mV), indicating that this channel was highly selective for Cl^-.

To further test the Cl^- selectivity of these channels, unitary Cl^- currents were recorded in the presence of different Cl^- concentrations in the *trans* chamber. Figure 1*B* shows the current-voltage (I-V) relations from 3 experiments where the *trans* Cl^- concentration was raised from 50 to 350 mM while the *cis* Cl^- concentration was maintained at 350 mM. In all ionic conditions, E_{rev} was within 1 mV of E_{Cl^-}. For each condition, permeability ratios for K^+ (P_{K^+}/P_{Cl^-}) were estimated from a form of the Goldman-Hodgkin-Katz (GHK) equation:

$$E_{rev} = \frac{RT}{F} \ln \frac{(P_{K^+}/P_{Cl^-}) \times [A_{K^+}]_o + [A_{Cl^-}]_i}{(P_{K^+}/P_{Cl^-}) \times [A_{K^+}]_i + [A_{Cl^-}]_o}$$

where P_{K^+} and P_{Cl^-}, are the absolute permeabilities for K^+ and Cl^-, respectively, and A_{K^+} and A_{Cl^-} are the activities of K^+ and Cl^-, respectively (Robinson & Stokes, 1968). The permeability ratios obtained for the 3 different experimental conditions with asymmetric KCl concentrations (50, 150, and 250 mM KCl *trans*) were averaged. The mean permeability ratio for K^+, P_{K^+}/P_{Cl^-}, was 0.012, indicating that these channels are ~80 fold selective for Cl^- over K^+. Similar experiments with NaCl instead of KCl showed that P_{Na^+}/P_{Cl^-} ~ 0.04 (*data not shown*).

A prominent feature of these Cl^- channels was the existence of two conductance substates. Transitions to these substates were observed in all our experiments (e.g., Fig. 1*A*, top record). Figure 2*A* shows single-channel recordings in symmetrical 250 mM KCl with transitions to substates with conductances corresponding to ~50 and 120% of the main open state (*O*). Transitions to the 50% substate (S_1) occurred at all voltages and were generally initiated from the main open state. Their durations varied from a few msec to several hundreds of msec. Under asymmetrical conditions, when *trans* Cl^- varied from 50 to 250 mM, the 50% substate exhibited a selectivity for chloride that was similar to that of the main conductance level (*data not shown*). Transitions to the 120% substate (S_2) also originated from the main conductance level and occurred at all voltages, but their durations were brief. The current amplitude histogram shown in Fig. 2*B* shows the amplitude of the various conductance states, *O*, S_1, and S_2 in symmetrical 250 mM Cl^- at +60 mV. The histogram was fitted to the sum of 3 Gaussian distributions. The calculated mean currents for *C*, S_1 and *O* were 0, 3.9, and 7.9 pA, respectively. Because transitions to S_2 were too brief to yield a good amplitude distribution, the histogram data corresponding to that substate was not fitted. Current-voltage relations for these 3 conductance states are shown in Fig. 2*C*. All relations were linear over the –20 – +80 mV voltage range. In symmetrical 250 mM Cl^-, the main open state conductance was 130 pS and the conductances of the two substates were 61 and 154 pS.

Concentration Dependence of Single-Channel Conductance

To determine the affinity with which Cl^- interacts with the channel pore, and to provide a means to compare the conductance of these channels with others measured at other ionic conditions, single-channel conductance was measured in various Cl^- concentrations. *Cis* and *trans* Cl^- concentrations were raised from 200 mM to 2 M and

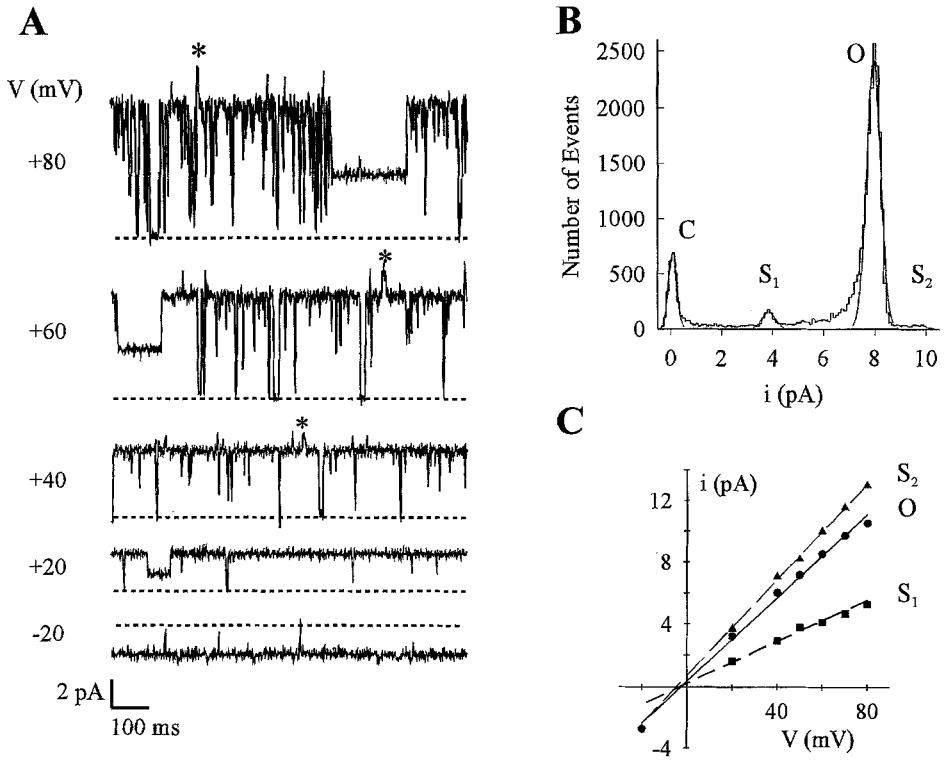

Fig. 2. Channel conductance states in symmetrical 250 mM KCl. (*A*) Typical single-channel recordings in symmetrical 250 mM KCl. The symbols (*) indicate transitions to the S_2 conductance substate. (*B*) Current-amplitude histogram, $V = +60$ mV; *O*, main conductance level, S_1 and S_2, substates; *C*, closed level. Data were fitted to the sum of 3 Gaussian functions. (*C*) Current-voltage relations in symmetrical 250 mM KCl. (■) 61 pS substate, (●); main open state, 130 pS; (▲), 154 pS substate. Data from 1 experiment.

single-channel current amplitudes were measured at various voltages for each concentration. Channel conductance was determined from the slope of the current-voltage curves and plotted *vs.* Cl^- activity. Figure 3 shows the results pooled from 4 experiments. Conductance increased with Cl^- activity and reached saturation around 1 M. The data was well-fit by a Michaelis-Menten equation, with a K_m of 543 mM activity (equivalent to 900 mM in concentration units) and a maximum conductance of 488 pS. These parameters differ from those reported for other SR Cl^- channels (*see* Discussion). The finding of conductance saturation indicates that there is at least one saturable step in ion conduction, and is consistent with the presence of at least one low-affinity ion-binding site in the conduction pathway.

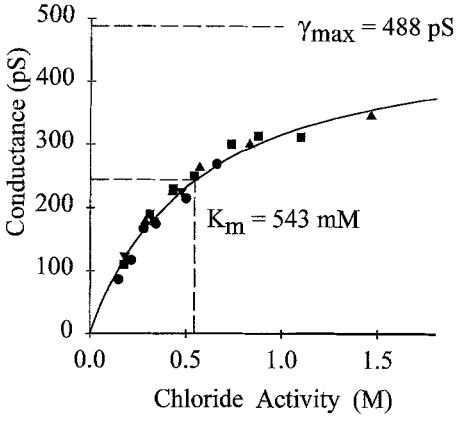

Fig. 3. Single-channel conductance in various symmetrical Cl^- concentrations. Single-channel currents were recorded in symmetrical Cl^- concentrations ranging from 200 mM to 2 M. Conductance was obtained from individual current-voltage curves and plotted *vs.* Cl^- activity. Activity coefficients were obtained from Robinson and Stokes (1968). Results are from 4 experiments, with each symbol type representing data from one experiment. Data points were fitted to the Michaelis-Menten equation: $\gamma = \gamma_{max}/(1 + K_m/A_{Cl^-})$; where γ is the conductance; γ_{max}, the maximal conductance; and K_m, a measure of the affinity with which Cl^- interacts with the channel pore, corresponds to the Cl^- activity (A_{Cl^-}) at which $\gamma = \gamma_{max}/2$. The K_m of 543 mM (activity) corresponds to 900 mM (concentration).

Permeability to Anions

To determine which anions can permeate this channel, permeability to various anions was tested. In some experiments, the *cis* chamber contained 250 mM Cl^- and the *trans* chamber had the same concentration of the test anion and no Cl^-. In other experiments, because of bilayer instability or because channel incorporation was difficult in the absence of *trans* Cl^-, the *trans* chamber

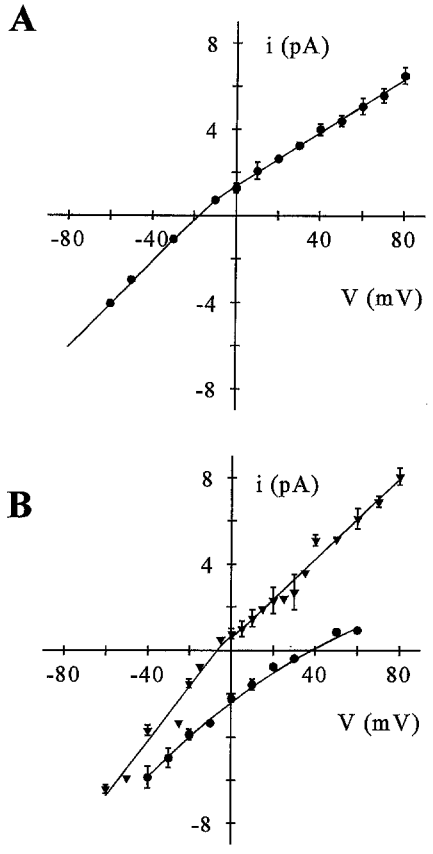

Fig. 4. Current-voltage relations showing SCN^- and I^- selectivity over Cl^-. (*A*) Single-channel amplitudes were measured in the presence of 250 mM NaCl *cis* and 250 mM NaSCN *trans*. E_{rev} of −18 mV indicated that $P_{SCN^-}/P_{Cl^-} = 2.15$. (*B*) Single-channel amplitudes were first measured in the presence of 250 mM NaCl *cis* and 50 mM NaCl *trans* (●). Addition of 200 mM NaI *trans* (▼) shifted E_{rev} from ~ +40 to ~ −5 mV, indicating that $P_{I^-}/P_{Cl^-} = 1.31$. Data points are means ± SD from 3 experiments.

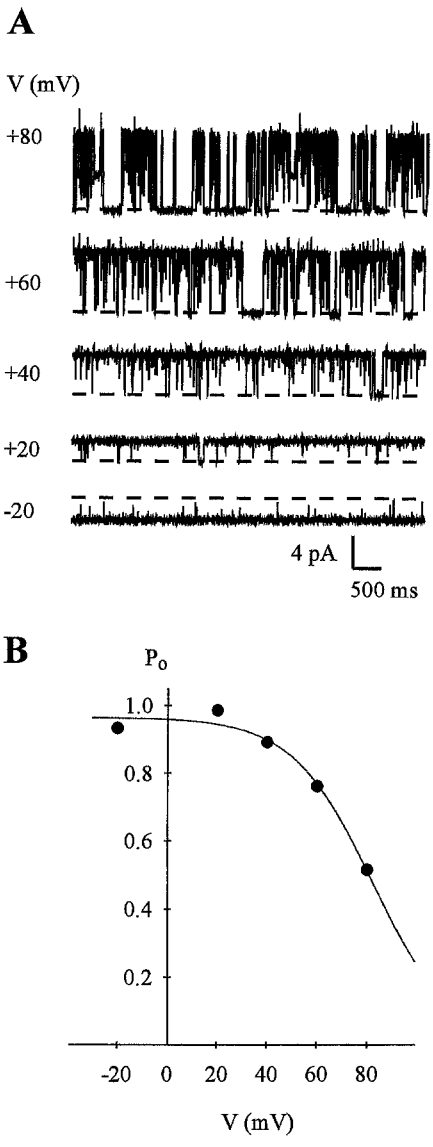

Fig. 5. Channel open probability (P_o) at different membrane voltages. (*A*) Single-channel currents were recorded in symmetrical 250 mM KCl. (*B*) Each point represents the P_o from ~1 min of recording. Results from one experiment. Data were fitted to the Boltzmann distribution:

$$P_o = \frac{P_{o\,/\max}}{1 + e^{(z(V_{1/2} - V)F/RT)}}$$

where $P_{o,\,max}$ is the maximum P_o, z is the gating charge, V is the membrane voltage, and $V_{1/2}$ the voltage at which $P_o = 0.5$. The best fit gave $P_{o,\,max} = 0.96$, $V_{1/2} = +82$ mV, and $z = 1.58$. The means ± standard deviations of $P_{o,\,max}$, $V_{1/2}$, and z values from eleven such analyses were 0.985 ± 0.026, +83.5 ± 12.6 mV, and 1.37 ± 0.57, respectively.

contained 50 mM Cl^-, and after channel incorporation, 200 mM of the test anion was added to this chamber. In both cases, reversal potentials and selectivity ratios were determined from current-voltage relations. Figure 4*A* shows the I-V curve obtained from pooling data from 3 experiments with 250 mM Cl^- *cis* and 250 mM thiocyanate *trans*. The reversal potential, E_{rev}, was ~ −18 mV, indicating that thiocyanate was more permeant than Cl^-. Figure 4*B* shows the I-V curves obtained from 3 experiments with 250 mM Cl^- *cis* and 50 mM Cl^- *trans*, and after addition of 200 mM iodide *trans*. Addition of iodide shifted E_{rev} from ~ +40 mV to ~ −5 mV, indicating that iodide was also more permeant than Cl^-. Permeability ratios for halide anions and several polyatomic anions were calculated from reversal potential measurements and the GHK equation. Because P_{K^+}/P_{Cl^-} and P_{Na^+}/P_{Cl^-} were very small, the permeabilities of K^+ and Na^+ were assumed to be zero in our calculations. The sequence of relative permeabilities for the tested anions is SCN^- (2.15) > I^- (1.31) > NO_3^- (1.22) ~ Br^- (1.21) > Cl^- (1.00) > F^- (0.81) > $HCOO^-$ (0.53). Larger anions, such as acetate and propionate were not permeant. The permeability sequence suggests that permeant ions interact with a cationic site of low field strength within the channel pore (Wright & Diamond, 1977).

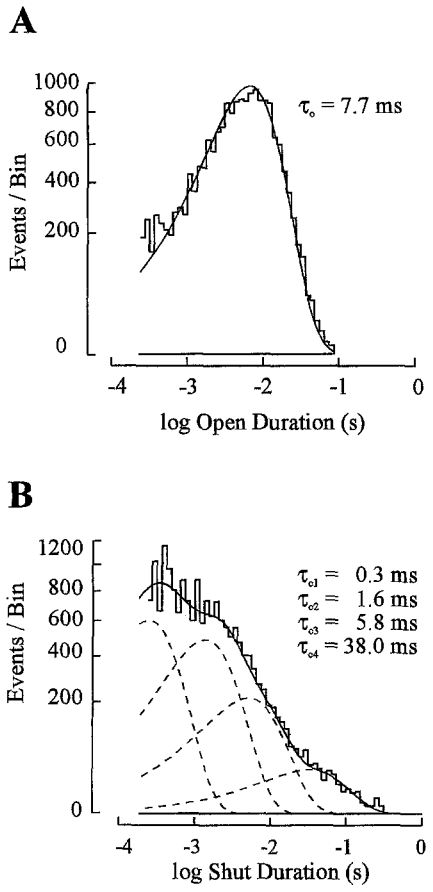

Fig. 6. Open (*A*) and shut (*B*) intervals distributions at +60 mV. Open and closed times intervals were obtained from single-channel recordings filtered at 1 kHz and digitized at 25 kHz. The open-time distribution was well-fit by a single exponential function with a mean of 7.7 msec. The closed-time distribution was best fit by the sum of 4 exponential functions with means equal to 0.3, 1.6, 5.8, and 38 msec. Data from one experiment.

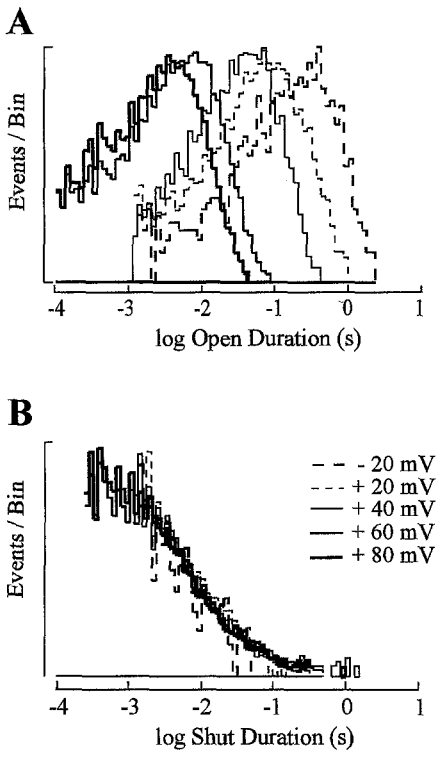

Fig. 7. Open (*A*) and shut (*B*) intervals distributions at various holding potentials. Intervals were obtained from single-channel recordings filtered at 200 Hz (−20 and +20 mV), 500 Hz (+40 mV), or 1 kHz (+60 and +80 mV) and digitized at 25 times the filter frequency. Open and closed times histograms were scaled to the same maximum. (*A*) Each histogram could be fitted to a single exponential distribution. Mean open times were: 4.3 msec (+80 mV), 7.7 msec (+60 mV), 51 msec (+40 mV), 110 msec (+20 mV), and 323 msec (−20 mV). (*B*) Each distribution could be fitted by the sum of several exponential functions (*see* previous figure). Data from 1 experiment (same experiment in *A* and Fig. 6).

Voltage Dependence of Single-Channel Gating

The recordings shown in Fig. 2*A* suggest that transitions between the open and the closed state vary with membrane voltage. Around 0 mV and at negative voltages the channel was open most of the time, and transitions to the closed state were rare. In contrast, channel gating was faster at large positive potentials (e.g., at +60 and +80 mV). This behavior is seen more clearly on a compressed time scale (Fig. 5*A*). To further characterize channel sensitivity to membrane voltage, we examined channel open probability (P_o), open times, and closed times as a function of membrane voltage.

Figure 5*B* shows the relation between channel P_o and membrane voltage. P_o was high ($P_{o,max}$ ~ 1) from −20 to +40 mV, and decreased to ~0.5 at +80 mV. Fitting the data to a Boltzmann distribution (*see* figure legend) revealed a maximum value for P_o ($P_{o,max}$) of 0.96, a voltage at which P_o is half-maximal ($V_{1/2}$) of +82 mV, and indicated that the transition from the closed to the open state was a conformational change involving ~1 gating charge (z = 1.58). Similar analysis for 11 experiments gave $P_{o,max}$ = 0.985 ± 0.026, $V_{1/2}$ = +83.5 ± 12.6 mV, and z = 1.37 ± 0.57 (mean ± SD). Open probability of these channels was independent of calcium levels in the *cis* or *trans* chambers (10 nM to 1 mM, *data not shown*).

To determine whether open and closed intervals vary with voltage, open and shut interval distributions were constructed from data acquired at different holding potentials. Examples of open and closed times distributions at +60 mV are shown in Fig. 6. The open interval distribution (Fig. 6*A*) was well-described by a single exponential (τ_o ~ 8 msec), but fitting the closed intervals distributions (Fig. 6*B*) required four exponential components, indicating that the channel entered at least four closed states. To compare interval distributions obtained at different voltages, open and closed times histograms were scaled to the same maximum and superimposed

Table 2. Mean open and shut intervals at various holding potentials

Time constant	−20 mV	+20 mV	+40 mV	+60 mV	+80 mV
τ_o	338.0 ±21.2	155.3 ±66.0	47.9 ±17.1	12.0 ± 6.0	5.8 ± 1.8
τ_{c1}	.38 ± .02	.65 ± .01	.41 ± .08	.24 ± .05	.27 ± .05
τ_{c2}	2.10 ± 2.8	3.15 ± .07	1.82 ± .75	1.25 ± .4	1.19 ± .35
τ_{c3}	19.1 ±11.1	18.5 ± 2.1	10.2 ± 5.3	5.6 ± 1.41	6.41 ± 1.37
τ_{c4}			103.5 ±30.4	55.5 ±39.8	53.8 ±28.4

Mean open (τ_o) and closed times (τ_{c1-4}) were derived from fits of open and shut intervals distributions, *see* text and Figs. 6, 7. Data shown are means ± SD from 3–5 experiments.

(Fig. 7). Superimposing the open interval distributions for different voltages shows that open durations varied greatly with membrane voltage, with mean open times ranging from 323 msec at −20 mV to 4.3 msec at +80 mV (Fig. 7*A*). On the other hand, closed durations did not seem to be significantly affected by voltage (Fig. 7*B*). The results from 3–5 similar experiments are summarized in Table 2. Mean open times varied substantially with voltage, from ~340 msec at −20 mV to ~6 msec at +80 mV. Because channel transitions to the closed state were less frequent around 0 mV and because long closing events were rare at all voltages, shut intervals distributions at +20 and −20 mV were best fit by the sum of 3 exponential components. Although there was a trend towards shorter closed durations as the voltage was made more positive, the changes were not monotonic or significant. Therefore, the change in P_o observed between −20 and +80 mV (Fig. 5*B*) can be solely explained by a change in channel open time.

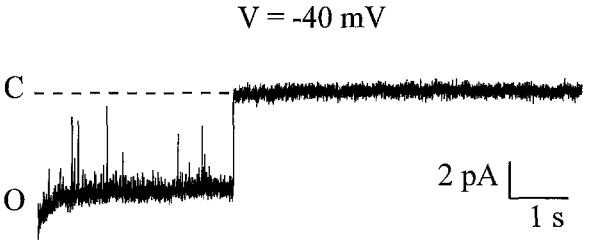

Fig. 8. Example of recordings at negative voltages. Channel activity was recorded in symmetrical 250 mM KCl immediately after a voltage step from 0 to −40 mV. The channel shut after ~3.4 sec at −40 mV. The broken line represents the closed level.

Although channel gating at voltages from −20 to +80 mV was stationary, we found that at −40 mV or below, channel activity was usually very high for a few seconds, and then the channel entered a long-lasting closed state. Most of the time, activity could be recov-

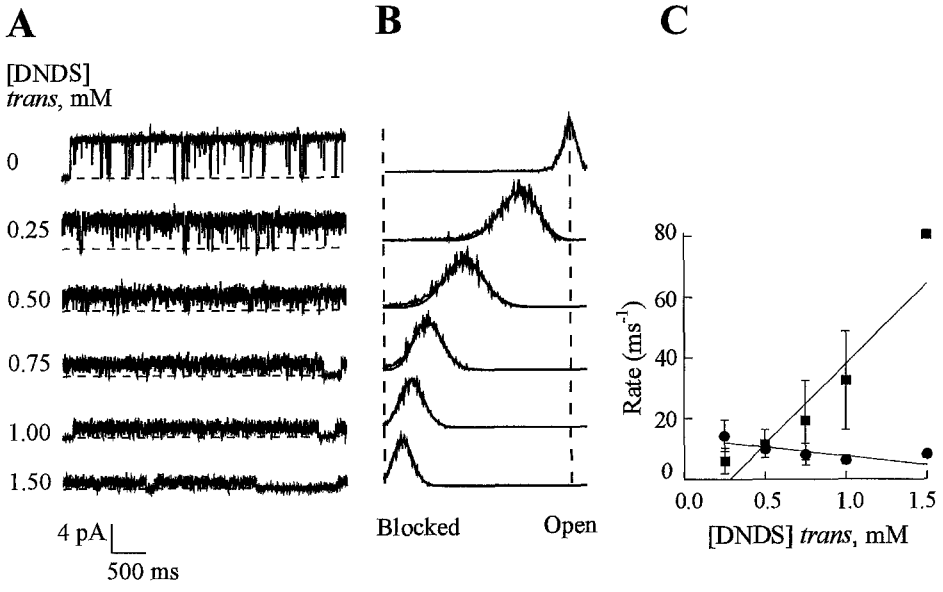

Fig. 9. Single-channel recordings at different concentrations of DNDS in the *trans* chamber (*A*). Single-channel currents were recorded in symmetrical 250 mM Cl^-, V = +40 mV. The broken lines represent the closed levels. (*B*) Current amplitude histograms for the different [DNDS] shown in (*A*). Continuous lines represent fits to the beta distribution (*see* Materials and Methods). (*C*) DNDS concentration dependence of blocking (■) and unblocking (●) rate constants. The lines represent the least-squares fit of the data. Values are means ± SD from 3 experiments.

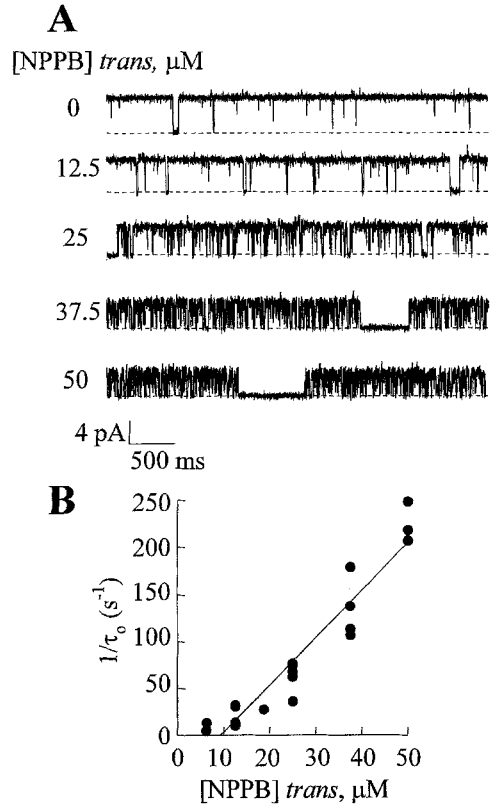

Fig. 10. Single-channel recordings at various concentrations of NPPB *trans* (*A*). Single-channel currents were recorded in symmetrical 250 mM Cl^-, V = +40 mV. The broken lines represent the closed levels. (*B*) NPPB concentration dependence of reciprocal open time constants. Data pooled from 6 experiments. For open time analysis, the filter frequency was 500 Hz and the sample rate 12.5 kHz. The lines represent the least-squares fit of the data.

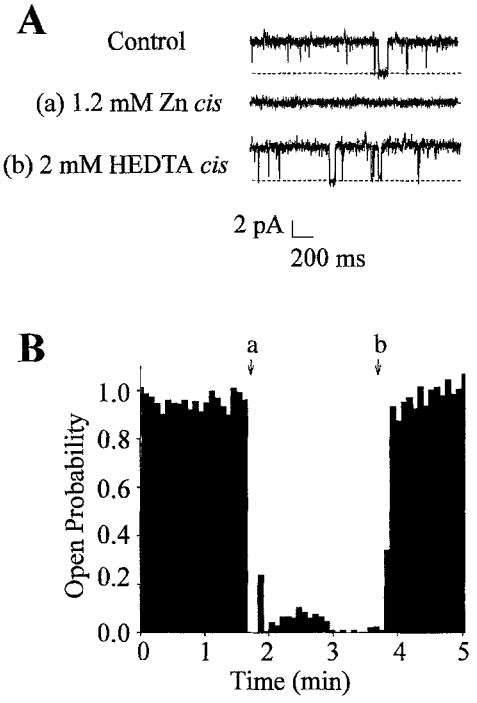

Fig. 11. Reversible block of Cl^- currents by zinc. (*A*) Single-channel recordings under control conditions, and (*a*) immediately after addition of zinc *cis*, (*b*) after chelating Zn^{2+} with HEDTA *cis*. Single-channel currents were recorded in symmetrical 250 mM Cl^-, V = +40 mV. (*B*) Channel open probability, same experiment, V = +40 mV.

ered by stepping to large positive potentials (+60 or +80 mV). Figure 8 shows an example of this behavior. After stepping from 0 to −40 mV, channel P_o was high for ~3.4 sec, and then the channel entered a long-lasting closed state. The channel did not reopen for the next 15 sec, until the voltage was changed to +80 mV. Channel activity then reappeared within 20 msec and the P_o returned to a stable level of 0.5. In several experiments, however, once the channel entered the long-lasting close state at −40 mV or below, its activity was never recovered again at any voltage. Because of this phenomenon, we could not evaluate stationary P_o or dwell times at voltages below −20 mV.

Channel Block by Disulfonic Stibenes, Arylaminobenzoates, and Divalent Cations

To compare the pharmacological properties of these voltage-sensitive channels with those of other Cl^- channels, the effects of various Cl^- channel blockers were tested.

Figure 9 shows the effect on single-channel behavior of a disulfonic stilbene, DNDS, on the *trans* side. DNDS decrease single-channel current amplitude is a dose-dependent manner. This block was observed at all voltages. Blocking and unblocking rate constants were obtained from fits of amplitude histograms with a beta distribution (Fig. 9*B*, *see* Methods). Figure 9*C* shows the concentration-dependence of these rate constants. The blocking rate increased with DNDS concentration from ~10 to ~80 $msec^{-1}$ whereas the unblocking rate remained almost constant around 10 $msec^{-1}$. The equilibrium dissociation constant (K_D) calculated from these rate constants was 415 μM. A similar value for DNDS block was obtained from the analysis of heavily-filtered single-channel current amplitudes (K_i = 570 μM, *not shown*). These results suggest that DNDS acts as a fast open channel blocker. Similarly, channel activity was blocked by other disulfonic stilbenes, including DIDS and SITS (*not shown*).

As shown in Fig. 10*A*, the arylaminobenzoate NPPB caused a dose-dependent increase in the frequency of current transitions between the open and closed state when added to the *trans* chamber. Kinetic analysis revealed that NPPB caused a dramatic decrease in channel mean open time, with an on rate (k_{on}) of 5.04 $\mu M^{-1} \cdot sec^{-1}$ (Fig. 10*B*). Because of the complexity of the shut intervals distributions (3–4 exponential components), no clear

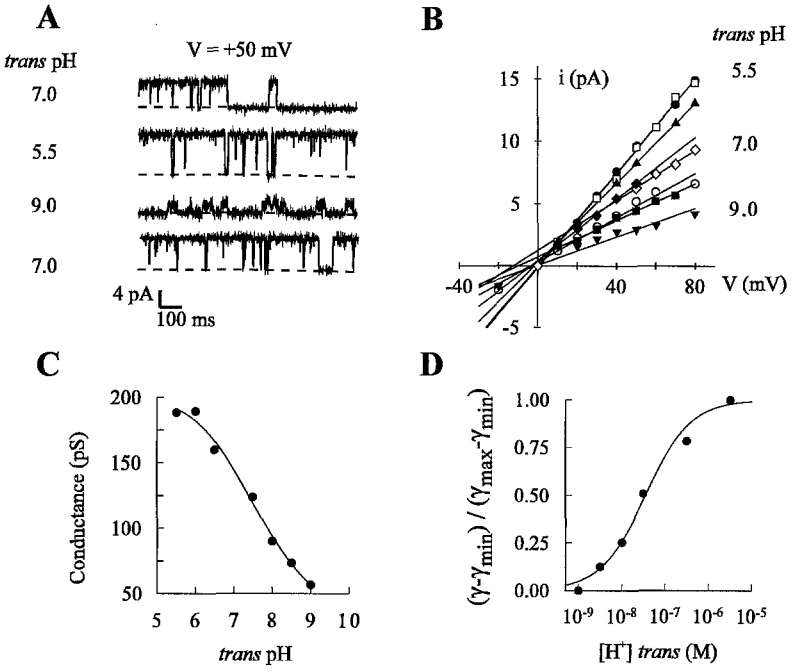

Fig. 12. Changes in pH *trans* affect single-channel conductance. (*A*) Single-channel events were recorded in symmetrical 250 mM Cl^-, 10 mM Bis-Tris-propane-MES, pH 7.0 at +50 mV. *Trans* pH was changed by addition of HCl or NaOH in the *trans* chamber, *cis* pH was constant at 7.0. (*B*) Current-voltage relations at *trans* pHs of 5.5 (●), 6.0 (□), 6.5 (▲), 7.0 (◇), 7.5 (♦), 8.0 (○), 8.5 (■), and 9.0 (▼). (*C*) Single-channel conductance at various *trans* pH values. (*D*) pH-dependent change in single-channel conductance. Conductance was normalized to the maximal increase in conductance and plotted *vs. trans* $[H^+]$. Data points were fitted to the Hill equation (*see* text). Data from one experiment.

effect of NPPB on closed times could be directly observed, and the off rate for NPPB could not be directly determined. NPPB decreased channel open probability with a K_i of 52.6 μM (*not shown*). Assuming simple bimolecular block by NPPB of the channel, and equivalence between K_i and K_D, we estimate the off rate of NPPB block to be around 265 sec^{-1}. Related compounds, anthracene-9-carboxylic acid and diphenylamine-2-carboxylate also blocked channel activity in a similar fashion, with K_is of 1500 and 707 μM, respectively (determined from open probability, *not shown*).

Several Cl^- channels are blocked by the divalent cations zinc and cadmium (Bretag, 1987). When added *cis* or *trans*, ~1 mM zinc caused a complete block of channel activity (Fig. 11). This effect could be readily reversed by the addition of a chelator, HEDTA, *cis* or *trans*. Similar results were obtained with cadmium (*not shown*).

pH Dependence of Single-Channel Conductance

To test channel sensitivity to pH over a wide range of pH values, single-channel currents were recorded in the presence of 10 mM Bis-Tris-propane buffered to pH 7.0 with MES (2-[N-morpholino]ethanesulfonic acid). pH was decreased or increased by addition of either 1 N HCl or 3 M NaOH *cis* or *trans*. Changing the pH in the *cis* chamber from 5.5 to 9.0 did not have any effect on single-channel behavior (*not shown*). However, altering the pH on the *trans* side had a large impact on the single-channel conductance. Figure 12 shows the results from an experiment where *trans* pH was changed over the range from 5.5 to 9.0. As shown in Fig. 12*A*, when *trans* pH was lowered from 7.0 to 5.5, unitary Cl^- current amplitudes increased from 6.4 pA to 9.6 pA. The subsequent increase in pH to 9.0 caused a decrease in unitary current amplitudes to 2.8 pA. This effect was completely reversible and returning to pH 7.0 caused single-channel current amplitudes to return to ~7 pA. Single-channel currents were measured at various voltages to construct current-voltage curves (Fig. 12*B*). Channel conductance was determined from the slope of these curves and plotted as a function of *trans* pH (Fig. 12*C*). Conductance was high at acidic pHs (~190 pS at pH 5.5), and decreased to ~60 pS at pH 9.0. The pH dependent change in single-channel conductance was normalized to the maximal change in conductance and plotted *vs. trans* $[H^+]$ (Fig. 12*D*). It was then fitted to the Hill equation:

$$(\gamma - \gamma_{min})/(\gamma_{max} - \gamma_{min}) = 1/(1 + (K_D/10^{-pH})^n)$$

where γ is the conductance; γ_{min} the conductance at pH 9.0; γ_{max}, the conductance at pH 5.5; K_D the $[H^+]$ at the half-maximal increase in conductance; and n, the Hill coefficient. The relationship between $[H^+]$ and the change in conductance was fitted by the equation with a Hill coefficient of 0.82 and a K_D corresponding to pH 7.4. The values for n and K_D resulting from pooling 3 such experiments were 0.76 and 5.73×10^{-8} M (pH 7.24), respectively.

Although there does appear to be an effect of pH on single-channel gating at pH 9.0 (Fig. 12*A*), no changes in open probability, open-times, or closed-times could be detected from a detailed analysis of the data at *trans* pHs

ranging from 5.5 to 8.5. At pH 9.0, the single-channel currents were small and channel openings were not well resolved, so a quantitative analysis of the changes in gating observed at this pH could not be done. Given the lack of effect on gating at pH 5.5–8.5, we conclude that the channel gating is not sensitive to pH, except possibly at the extremes.

Discussion

We report here the single-channel properties of a novel type of Cl^- channel from cardiac sarcoplasmic reticulum. We have examined its permeation properties, its voltage dependence, and its sensitivity to chloride channel blockers and pH.

Conductance and Selectivity

In many regards, Cl^- channels constitute a very heterogeneous family of ion channels. Their single-channel conductance varies between 1 and 500 pS, and they have been classified by some as low, intermediate, and high conductance (or maxi) Cl^- channels based on their conductance in 150 mM Cl^- (Fahlke, Zachlke, Zachar, & Rudel, 1992). Low conductance anion channels include channels with a conductance smaller than 30 pS, while intermediate conductance channels are those with a conductance between 30 and 200 pS, and maxi Cl^- channels correspond to 200–500 pS channels. The channels reported here have a single-channel conductance of 130 pS in symmetrical 250 mM Cl^- and of ~80 pS in 150 mM Cl^-. Therefore, they belong to the intermediate conductance group of Cl^- channels. Other intermediate conductance SR Cl^- channels have been reported. A 95 and a 55 pS channels have been observed in SR from skeletal and cardiac muscle, respectively (Rousseau et al., 1988; Rousseau, 1989). In addition, Kawano and coworkers (1992) reported a 71 pS Cl^- channel from cardiac SR. Other groups reported the observation of large conductance SR channels from rabbit skeletal muscle, including a 505 pS and a 200 pS channel in 200 and 100 mM Cl^-, respectively (Hals et al., 1989; Tanifuji et al., 1987). We did not observed any one of these previously described Cl^- channels in our experiments.

Like most ion channels, the channels reported here exhibit conductance substates. The two prominent substates have conductances around 50 and 120% that of the main conductance level. They follow the same ionic selectivity as the main conductance state. No transition to either substate was observed after the channel entered a long-lasting closed state, when the voltage was held below −40 mV. In addition, all 3 conductance states were observed in all of our experiments, and transitions to either substate were almost always initiated from the main conductance level. These observations support the idea that the 50 and 120% conductance levels are not distinct channels, but represent substates of the same channel protein.

Channel conductance increased with increasing Cl^- concentrations, reaching a maximum of ~500 pS around 2 M Cl^-. The data were well-described by a Michaelis-Menten relationship, with a maximal conductance, γ_{max}, of 488 pS and a K_m of ~900 mM concentration (543 mM in activity units). This indicates that there is a saturating step in ion conduction and that Cl^- interacts with at least one binding site in the pore. The K_m value indicates that Cl^- ions have a very low affinity for the channel pore. These values for γ_{max} and K_m are similar to those reported for a platelet Cl^- channel, with a K_m of 1008 mM and a γ_{max} of 503 pS, although the channel described in this report has distinct properties from the platelet channel (e.g., the platelet channel has a rectifying current-voltage relation and is insensitive to zinc; Manning & Williams, 1989). However, these parameters are different from those reported for other SR Cl^- channels. For rabbit skeletal muscle SR anion channels, Tanifuji et al. (1987) reported a maximal conductance of 700 pS and a K_m of 265 mM. Rousseau et al. (1988) reported a γ_{max} of 154 pS and a K_m of 125 mM. Hals et al. (1989) described a γ_{max} of 617 pS and a K_m of 77 mM.

The channel is very selective for Cl^- over small cations, but it is not especially selective among the anions tested. It displayed an anion conductivity sequence of SCN^- (2.15) > I^- (1.31) > NO_3^- (1.22) ~ Br^- (1.21) > Cl^- (1.00) > F^- (0.81) > $HCOO^-$ (0.53). The permeability ratios for halides follow Sequence 1 of Eisenman, namely $I^- > Br^- > Cl^- > F^-$, indicative of a low field strength cationic binding site (Eisenman, 1965; Wright & Diamond, 1977). The selectivity sequence reported here is similar to the partial sequence reported for a Cl^- channel from skeletal muscle SR (NO_3^- (1.3) > Br^- (1.2) > Cl^- (1.0); Tanifuji et al., 1987). But it differs from that reported by Hals et al. (1989) for a channel that is also from skeletal muscle SR (NO_3^- (1.53) > SCN^- (1.45) > I^- (1.39) > Br^- (1.00) = Cl^- (1.00)). It is similar to the sequences reported for some Cl^- channels from muscle, a neuronal Cl^- channel, and $GABA_A$- and glycine-receptor channels (Bormann, Hamill, & Sakmann, 1987; Franciolini & Nonner, 1987; Soejima & Kokubun, 1988; DeBin et al., 1994), but is different from those reported for some epithelial Cl^- channels, CFTR, and the Cl^- channel from *Torpedo* electroplax (Alton et al., 1991; Goldberg & Miller, 1991; Fuller & Benos, 1992; Preston, Calenzo, & Dubinsky, 1992; Wilk Blaszczak, French, & Man, 1992).

Voltage Dependence

Cl^- channel activity was stable at voltages ranging from −20 to +80 mV. Channel open probability varied be-

tween ~1.0 around 0 mV and 0.5 at +80 mV. The voltage-dependence of P_o could be described by a Boltzmann distribution, with a maximal P_o of 1.0, a $V_{1/2} \sim +80$ mV, and a gating charge, z, of 1.37. This value for z is much smaller than those reported by Palade and coworkers for a Cl^- channel from rabbit skeletal muscle SR ($z = 12$) or for a muscle surface membrane Cl^- channel ($z = 4.3$) (Hals et al., 1989; Woll et al., 1987). It is similar to that reported by Hanke and Miller (1983) for the double-barreled chloride channel from *Torpedo* electroplax ($z = 1.1$).

Stepping to voltages more negative than −20 mV caused the channel to enter a long-lasting closed state within seconds. P_o, however, remained high (~1) until the channel entered the long-lasting closed state. Sometimes the channel could be reactivated by stepping to large positive potentials (+60 or +80 mV), but entry into the long-lasting closed state at negative voltages was not always reversible. A similar channel has been observed for other Cl^- channels, although this asymmetry in the voltage-dependence of P_o is uncommon. For example, Blatz and Magleby (1983) reported the observation of a Cl^- channel from myotubes that was active at 0 mV but inactivated within seconds after voltage steps to either positive or negative voltages. This phenomenon, however, was fully reversible upon returning to 0 mV.

Open and shut interval analysis revealed that the channels can enter at least one open state and four closed states. Interestingly, open times but not closed times were significantly affected by membrane voltage. Open times varied from ~6 msec at +80 mV to several hundreds of msec at −20 mV. For most voltage-sensitive Cl^- channels, however, an increase in closed intervals duration is usually observed when P_o decreases. For example, Rousseau (1989) described a Cl^- channel from cardiac SR with an attenuated bell-shape voltage-dependence where the observed change in P_o was due to changes in the duration of both long closed times and open times.

Block

In this study, the effects of several types of Cl^- channel blockers were studied in order to characterize the channel pharmacologically. There are several classes of Cl^- channel blockers. They include inorganic blockers such as the anions I^-, SCN^-, I^-, Br^-, NO_3^-, and ClO_4^-, and the cations Zn^{2+}, Cd^{2+}, and Cu^{2+}, as well as various organic compounds, including disulfonic stilbenes derivatives, arylaminobenzoates, and phenoxyacetates (Bretag, 1987).

We tested the effects of three disulfonic stilbene derivatives on single-channel activity. DIDS, SITS, or DNDS partially blocked the channels in the 100–1500 μM range. This is consistent with the observation that micromolar to millimolar concentrations of disulfonic stilbenes can block Cl^- fluxes across the SR membrane as well as several SR Cl^- channels (Kasai, 1981; Smith, Coronado, & Meissner, 1986; Rousseau et al., 1988; Rousseau, 1989; Kawano et al., 1992).

We tested the effect of compounds belonging to other classes of anion channels blockers. The arylaminobenzoates NPPB, A-9-C, and DPC effectively blocked channel activity, inducing rapid transitions between open and closed levels. NPPB was the most potent blocker, with a K_i of 52.6 μM. Cromolyn, an antiallergic drug, was reported to block Cl^- channels from colonic carcinoma cells, with an K_i of 19 μM (Reinsprecht et al., 1992). In our studies, higher concentrations of cromolyn (>100 μM *trans*) were required to partially block channel activity (*not shown*). Niflumic acid, a well-known blocker of calcium-dependent Cl^- channels (White & Aylwin, 1990), did not have any effect on channel activity (up to 1 mM *cis* and *trans, not shown*). The channel was also insensitive to the scorpion venom toxin chlorotoxin (up to 800 nM *cis* and 600 nM *trans;* DeBin, Maggio, & Strichartz, 1993).

Several divalent ions such as zinc or cadmium can also act as Cl^- channel blockers (Bretag, 1987). Millimolar concentrations of zinc or cadmium completely blocked channel activity when added *cis* or *trans*. This effect was reversed when Zn^{2+} or Cd^{2+} were chelated with HEDTA. There is no other report of the effect of these cations on SR Cl^- conductance. But both cations, especially zinc, have been reported to reversibly block Cl^- conductance in various tissues, including channels from skeletal muscle (Hutter & Warner, 1967), smooth muscle (Kokubun, Saigusa, & Tamura, 1991), liver mitochondria (Selwyn, Ng, & Choo, 1993), and hippocampal GABA channels (Legendre & Westbrook, 1991). Studies on zinc-dependent enzymes indicate that cysteine and histidine residues may be involved in zinc binding. On the frog muscle Cl^- channel and on the lobster GABA channel, histidine residues were proposed as zinc binding sites, based on pH sensitivity (Hutter & Warner, 1967; Smart & Constanti, 1982).

pH Dependence

Channel conductance was very sensitive to *trans* pH. When *trans* pH was changed from 7.0 to 5.5, single-channel current was increased by ~50%, and when pH was increased to pH 9.0 (from 7.0), the current was decreased by ~50%. Changes in *cis* pH did not have any effect. These results can be interpreted as an effect on the protonation state of a specific amino acid that is accessible from the *trans* side only. Fitting the data to a Hill relation revealed an apparent pK_a around pH 7.2, which does not correspond to any pK_a reported for amino acid side chains. This is expected, since in a complex

Table 3. Conductance and voltage-dependence of known SR chloride channels

Reference	SR source	Conductance and substates	Voltage dependence
Tanifuji et al., 1987	rabbit skeletal muscle	200 pS in 100 mM Cl, at least 4 substates γ_{max} = 700 pS, K_m = 265 mM	yes, but not characterized in detail
Rousseau et al., 1988	rabbit skeletal muscle	95 pS in 260 mM Cl, some substates γ_{max} = 154 pS, K_m = 125 mM	attenuated bell shape, P_o = 0.6 to 0.95 for $-60 < V < +60$ mV
Rousseau, 1989	dog heart	55 pS in 260 mM Cl, some substates	bell shape, $P_{o,max}$ at +10 mV
Hals et al., 1989	frog skeletal muscle (sarcoballs)	505 pS in 200 mm Tris-Cl, 266 and 125 pS substates γ_{max} = 617 pS, K_m = 77 mM	bell shape, P_o ~1 at 0 mV, 0.05 at ±25 mV
	rabbit skeletal muscle (liposomes)	490 pS in 150 mM Cl, numerous substates	no
	frog skeletal muscle (liposomes)	400 pS in 200 mM Cl	not determined
Larralde and Nasi, 1989	toad skeletal muscle	140 pS in 200 mM Cl, one substate	high P_o around 0 mV, longer closed times and inactivation at positive voltages
Ide et al., 1991	rabbit skeletal muscle (purified protein)	115 pS in 300 mM Cl	not determined
Kawano et al., 1992	pig heart	116 pS in 500 mM Cl and 71 pS in 250 mM Cl	no (−60 to +100 mV)
This report	pig heart	130 pS in 250 mM Cl, 60 and 155 pS substates γ_{max} = 488 pS, K_m = 900 mM	asymmetric, P_o = 1.0 around 0 mV, and 0.5 at ~+80 mV.

macromolecule with multiple charges and electrostatic influences, a given acid-base group may have a pK_a that varies by as much as several pH units from its expected value. Further studies with specific amino acid modifiers (e.g., histidine modification by diethylpyrocarbonate) would be necessary to identify the amino acid(s) involved in this phenomenon. Alternatively, the effect of pH on single-channel conductance can be interpreted as block of Cl^- currents by OH^- ions, with a K_i of 0.174 μM.

Several other anion channels are affected by pH. Halm and Frizzell (1992) reported that increasing intracellular pH from 6.0 to 9.0 reduced the single-channel conductance of an epithelial Cl^- channel by 40%. Hals and Palade (1990) reported that increasing luminal pH from 7.0 to 8.0 reduced the single-channel conductance of the sarcoball Cl^- channel from 505 to 257 pS and that the conductance of this channel was constant (505 pS) over the 4.0 to 7.0 pH range. Extracellular acidification was shown to decrease the open probability of CFTR channels by 47% (Sherry, Cuppoletti, & Malinowska, 1994) and to abolish the activity of Cl^- channels from gastric parietal cells (Cuppoletti, Baker, & Malinowska, 1993). Rousseau (1988, 1989) reported that Cl^- channels from skeletal and cardiac muscle SR were insensitive to changes in pH from 6.8 to 8.0 and 7.4 to 6.8, respectively. Yet it is unclear whether these were changes in *cis* or *trans* pH or whether conductance was one of the single-channel parameters examined under the different pH conditions. A change in *trans* pH from 6.8 to 8.0 would result in a ~30% decrease in conductance for the channel reported here.

This pH effect on Cl^- channel conductance may be functionally important. An acidification of the lumen of the SR would increase SR Cl^- conductance, whereas alkalinization would reduce it. It is unclear what pH changes, if any, take place during SR Ca^{2+} uptake or release. It is possible, however, that acidification may occur upon binding of Ca^{2+} to the highly acidic SR Ca^{2+} buffer protein calsequestrin (Yano & Zarain-Herzberg, 1994).

Comparison with Other Cl^- Channels

Because the channel reported here has some unique biophysical properties, including single-channel conductance, voltage-dependence, and pH dependence, we believe that it is different from previously reported SR Cl^- channels. Table 3 summarizes the conductance and voltage-dependent properties of previously described SR Cl^- channels from various preparations. Focusing on cardiac SR, the Cl^- channel characterized in this paper differs from the Cl^- channel reported by Rousseau (1989) in its conductance (130 pS *vs.* 55 pS in ~250 mM Cl^-), its voltage-dependence, and its pH sensitivity, as mentioned above. The Cl^- channel described in this pa-

per is also different from the channel described by Kawano et al. (1992) because of its conductance and voltage sensitivity (*see* Table 3). Regarding skeletal muscle, the Cl^- channel described here could be similar in conductance and gating to that from toad skeletal muscle SR (Larralde & Nasi, 1989; but *see* discussion below). It is substantially different from all of the other previously described Cl^- channels from skeletal muscle SR (*see* Table 3). These differences may arise from differences between skeletal muscle and cardiac muscle or may be attributed to the different species from which the SR was isolated.

On the other hand, it is possible that the different biophysical properties described in the various reports mentioned above arise from different experimental conditions, such as different lipid compositions of the bilayers. The Cl^- channel described here has a single-channel conductance that is in the same range as some of the previously reported SR Cl^- channels (*see* Table 3), and it is possible that small differences in conductance could arise from differences in membrane composition or other experimental details.

In addition, differences in the way data are analyzed may result in apparently different channel properties. For example, if we averaged channel open probabilities at negative voltages where the channel enters long-lasting closed states, we might observe a bell-shaped open probability *vs.* voltage relation (depending on the time spent at the negative voltages and the rate of entering the long-lasting closed state). Also, Larralde and Nasi (1989) have described in an abstract a Cl^- channel that tends to inactivate at positive voltages and not at negative voltages, but it is unclear from their abstract how voltage was defined in their studies and it is possible that differences in the voltage dependence between the channels may arise from different voltage conventions.

Because it is possible that this Cl^- channel comes from the surface membrane (but *see* the comments in Materials and Methods), it is useful to compare the properties of the channel with surface membrane Cl^- channels. In general, the Cl^- channel reported here differs from all cardiac surface membrane Cl^- channels described to date. These include Cl^- channels reconstituted from calf sarcolemma (Coronado & Latorre, 1982), large conductance Cl^- channels seen only in newborn rat myocytes (Coulombe et al., 1987), protein kinase A- and protein kinase C-activated Cl^- channels (Ehara & Ishihara, 1989; Collier & Hume, 1995), swelling-activated Cl^- channels (Coulombe & Coraboeuf, 1992), and outwardly-rectifying Cl^- channels (Duan & Nattel, 1994). Specifically, it differs from the channels described by Coronado and Lattore (1982) and Duan and Nattel (1994) because these channels exhibit nonlinear current-voltage relations under symmetrical conditions. The Cl^- channels found in newborn rat myocytes (Coulombe et al., 1987) have larger conductances (200–250 pS and 400–450 pS in ~160 mM Cl^-) than the one described here. Kinase-activated channels have a much smaller conductance (~10 pS in 150 mM Cl^-) and are insensitive to voltage changes or disulfonic stilbenes (Ehara & Ishihara, 1989; Collier & Hume, 1995). The channels described by Coulombe and Coraboeuf (1992), seen in blebs or after application of hyptonic media, also had a very large conductance (400 pS in symmetrical 150 mM Cl^-) and multiple conductance substates.

Conclusions

We have characterized a novel Cl^- channel from cardiac sarcoplasmic reticulum. This channel has an intermediate conductance, is very Cl^- selective, and is affected by membrane voltage and pH. It is likely to play an important role in the regulation of ion flow across the SR. It has been suggested that ionic fluxes through SR potassium and chloride channels may play a role during release or uptake of calcium by the SR as a pathway for counter ion movements, allowing faster calcium transients and a faster muscle contraction.

For example, the release of Ca^{2+} from the SR would tend to make the lumen of the SR negative with regard to the cytoplasm which would limit further rapid Ca^{2+} efflux. The negative voltage in the lumen corresponds to a positive cytoplasmic voltage and a positive voltage as defined by our experimental conditions (where voltages are defined as *cis* relative to *trans* or cytoplasmic relative to lumenal, assuming standard fusion of SR vesicles). This positive voltage would tend to decrease the P_o of the Cl^- channel described in this paper. However, the midpoint for the voltage dependence of P_o is quite positive (~ +80 mV) and channel activity would still be substantial during efflux of Ca^{2+}. Furthermore, other channels besides this Cl^- channel are present in the SR (e.g., SR K^+ channels) and their action would attenuate the voltage changes due to the release of Ca^{2+} and keep the transmembrane voltage difference close to 0 mV.

In addition, Ca^{2+} uptake in the SR during relaxation could also be electrogenic and lead to a voltage gradient across the SR membrane (i.e., lumenal positive). This would correspond to a shift towards negative voltages under our voltage convention and could possibly turn off Cl^- channel activity due to the long-lasting inactivation process. However, other channels such as the SR K^+ channel would help keep the voltage away from extremely negative voltages. Therefore, the action of the SR Cl^- channels described in this report is likely to be helpful in keeping voltage gradients across the SR membrane quite low to allow faster Ca^{2+} release and uptake in the SR.

We thank Dr. Barry Pallotta for help with open and closed intervals analysis and Dr. Gerhard Meissner for his suggestions for the prepa-

ration of cardiac sarcoplasmic reticulum membranes. This work was supported by a grant from the National Institutes of Health to R.L.R. and a Student Grant-in-Aid from the American Heart Association, North Carolina affiliate to C.T. R.L.R. is an Established Investigator of the American Heart Association.

References

Alton, E.W., Manning, S.D., Schlatter, P.J., Geddes, D.M., Williams, A.J. 1991. Characterization of a Ca(2+)-dependent anion channel from sheep tracheal epithelium incorporated into planar bilayers. *J. Physiol.* **443:**137–159

Anderson, K., Lai, F.A., Liu, Q.Y., Rousseau, E., Erickson, H.P., Meissner, G. 1989. Structural and functional characterization of the purified cardiac ryanodine receptor-Ca release complex. *J. Biol. Chem.* **264:**1329–1335

Blatz, A.L., Magleby, K.L. 1983. Single voltage-dependent chloride-selective channels of large conductance in cultured rat muscle. *Biophys. J.* **43:**237–241

Bormann, J., Hamill, O.P., Sakmann, B. 1987. Mechanism of anion permeation through channels gated by glycine and gamma-aminobutyric acid in mouse cultured spinal neurones. *J. Physiol.* **285:**243–286

Bretag, A.H. 1987. Muscle chloride channels. *Physiol. Rev.* **67:**618–724

Collier, M.L., Hume, J.R. 1995. Unitary chloride channels activated by protein kinase C in guinea pig ventricular myocytes. *Circ. Res.* **76:**317–324

Colquhoun, D., Sigworth, F.J. 1983. Fitting and statistical analysis of single-channel records. *In:* Single-channel recording. B. Sakmann and E. Neher, editors. pp. 191–263. Plenum Publishing, New York

Coronado, R., Lattore, R. 1982. Detection of K^+ and Cl^- channels from calf cardiac sarcolemma in planar lipid bilayer membranes. *Nature.* **298:**849–852

Coulombe, A., Coraboeuf, E. 1992. Large-conductance chloride channels of newborn rat cardiac myocytes are activated by hypotonic media. *Pflüegers Arch.* **422:**143–150

Coulombe, A., Duclohier, H., Coraboeuf, E., Touzet, N. 1987. Single chloride-permeable channels of large conductance in cultured cardiac cells of new-born rats. *Eur. Biophys. J.* **14:**155–162

Cuppoletti, J., Baker, A.M., Malinowska, D.H. 1993. Cl^- channels of the gastric parietal cell that are active at low pH. *Am. J. Physiol. Cell Physiol.* **264:**C1609–C1618

Darling, E.M., Lai, F.A., Meissner, G. 1992. Effects of regional ischemia on the ryanodine-sensitive Ca release channel of canine sarcoplasmic reticulum. *J. Mol. Cell. Cardiol.* **24:**1179–1188

DeBin, J.A., Maggio, J.E., Strichartz, G.R. 1993. Purification and characterization of chlorotoxin, a chloride channel ligand from the venom of the scorpion. *Am. J. Physiol. Cell Physiol.* **264:**C361–C369

DeBin, J.A., Wood, M.R., Pfenninger, K.H., Strichartz, G.R. 1994. A Cl^- channel reconstituted from fetal rat brain growth cones. *J. Membrane Biol.* **141:**7–19

Duan, D., Nattel, S. 1994. Properties of single outwardly rectifying Cl^- channels in heart. *Circ. Res.* **75:**789–795

Ehara, T., Ishihara, K. 1990. Anion channels activated by adrenaline in cardiac myocytes. *Nature.* **347:**284–286

Eisenman, G. 1965. Some elementary factors involved in specific ion permeation. *Proc. XXIIIrd Int. Congr. Phys. Sci.* **87:**489–506

Fabiato, A. 1983. Calcium-induced release of calcium from the cardiac sarcoplasmic reticulum. *Am. J. Physiol. Cell Physiol.* **245:**C1–C14

Fahlke, C., Zachar, E., Rudel, R. 1992. Single-channel recordings of chloride currents in cultured human skeletal muscle. *Pfluegers Arch.* **421:**108–116

Forbush, B. III. 1983. Assay of Na,K-ATPase in plasma membrane preparations: Increasing the permeability of membrane vesicles using sodium dodecyl sulfate buffered with bovine serum albumin. *Anal. Biochem.* **128:**159–163

Franciolini, F., Nonner, W. 1987. Anion and cation permeability of a chloride channel in rat hippocampal neurons. *J. Gen. Physiol.* **90:**453–478

Fuller, C.M., Benos, D.J. 1992. CFTR! *Am. J. Physiol. Cell Physiol.* **32:**C267–C286

Garcia, A.M., Miller, C. 1984. Channel mediated monovalent cation fluxes in isolated sarcoplasmic reticulum vesicles. *J. Gen. Physiol.* **83:**819–839

Goldberg, A.F., Miller, C. 1991. Solubilization and functional reconstitution of a chloride channel from Torpedo californica electroplax. *J. Membrane Biol.* **124:**199–206

Halm, D.R., Frizzell, R.A. 1992. Anion permeation in an apical membrane chloride channel of a secretory epithelial cell. *J. Gen. Physiol.* **99:**339–366

Hals, G.D., Palade, P.T. 1990. Different sites control voltage dependence and conductance of sarcoball anion channel. *Biophys. J.* **57:**1037–1047

Hals, G.D., Stein, P.G., Palade, P.T. 1989. Single-channel characteristics of a high conductance anion channel in "sarcoballs". *J. Gen. Physiol.* **93:**385–410

Hanke, W., Miller, C. 1983. Single chloride channels from Torpedo electroplax. Activation by protons. *J. Gen. Physiol.* **82:**25–45

Hutter, O.F., Warner, A.E. 1967. Action of some foreign cations and anions on the chloride permeability of frog muscle. *J. Physiol.* **189:**445–460

Ide, T., Sakamoto, H., Morita, T., Taguchi, T., Kasai, M. 1991. Purification of a Cl^- channel protein of sarcoplasmic reticulum by assaying the channel activity in the planar lipid bilayer system. *Biochem. Biophys. Res. Commun.* **176:**38–44

Jorgensen, A.O., Arnold, W., Pepper, D.R., Kahl, S.D., Mandel, F., Campbell, K.P. 1988. A monoclonal antibody to the Ca^{2+}-ATPase of cardiac sarcoplasmic reticulum cross-reacts with slow type I but not with fast type II canine skeletal muscle fibers: an immunocytochemical and immunochemical study. *Cell Motil. Cytoskel.* **9:**164–174

Kasai, M. 1981. Inhibition of the anion permeability of sarcoplasmic reticulum vesicles by some stilbenes derivatives. *J. Biol. Chem.* **89:**943–953

Kawano, S., Hiraoka, M. 1993. Protein kinase A-activated chloride channel is inhibited by the Ca^{2+}-calmodulin complex in cardiac sarcoplasmic reticulum. *Circ. Res.* **73:**751–757

Kawano, S., Nakamura, F., Tanaka, T., Hiraoka, M. 1992. Cardiac sarcoplasmic reticulum chloride channels regulated by protein kinase A. *Circ. Res.* **71:**585–589

Kokubun, S., Saigusa, A., Tamura, T. 1991. Blockade of Cl channels by organic and inorganic blockers in vascular smooth muscle cells. *Pfluegers Arch.* **418:**204–213

Korn, S.J., Horn, R. 1988. Statistical discrimination of fractal and Markov models of single-channel gating. *Biophys. J.* **54:**871–877

Larralde, L., Nasi, E. 1989. A voltage-dependent anionic channel from the sarcoplasmic reticulum of *Bufo marinus* reconstituted in planar lipid bilayers. *Biophys. J.* **55:**321*a.* (*Abst.*)

Legendre, P., Westbrook, G.L. 1991. Noncompetitive inhibition of gamma-aminobutyric acid A channels by Zn. *Mol. Pharmacol.* **39:**267–274

Magleby, K.K. 1992. Preventing artifacts and reducing errors in single-channel analysis. *Methods Enzymol.* **207:**763–791

Manning, S.D., Williams, A.J. 1989. Conduction and blocking prop-

erties of a predominantly anion-selective channel from human platelet surface membrane reconstituted into planar phospholipid bilayers. *J. Membrane Biol.* **109:**113–122

McManus, O.B., Magleby, K.L. 1988. Kinetic states and modes of single large-conductance calcium-activated potassium channels in cultured rat skeletal muscle. *J. Physiol.* **402:**79–120

Meissner, G. 1983. Monovalent ion and calcium ion fluxes in sarcoplasmic reticulum. *Mol. Cell. Biochem.* **55:**65–82

Meissner, G., McKinley, D. 1982. Permeability of canine cardiac sarcoplasmic reticulum vesicles to K, Na, H, and Cl. *J. Biol. Chem.* **257:**7704–7711

Miller, C. 1978. Voltage-gated cation conductance channel from fragmented sarcoplasmic reticulum: steady-state electrical properties. *J. Membrane Biol.* **40:**1–23

Preston, C.L., Calenzo, M.A., Dubinsky, W.P. 1992. Isolation of a chloride channel-enriched membrane fraction from tracheal and renal epithelia. *Am. J. Physiol. Cell Physiol.* **263:**C879–C887

Reinsprecht, M., Pecht, I., Schindler, H., Romanin, C. 1992. Potent block of Cl^- channels by antiallergic drugs. *Biochem. Biophys. Res. Commun.* **188:**957–963

Ríos, E., Pizarro, G. 1991. Voltage sensor of excitation-contraction coupling in skeletal muscle. *Physiol. Rev.* **71:**849–908

Robinson, R.A., Stokes, R.H. 1968. Electrolyte solutions. Butterworths, London

Rosenberg, R.L., Chen, X. 1991. Characterization and localization of two ion-binding sites within the pore of cardiac L-type calcium channels. *J. Gen. Physiol.* **97:**1207–1225

Rosenberg, R.L., Hess, P., Tsien, R.W. 1988. Cardiac calcium channels in planar lipid bilayers. L-type channels and calcium-permeable channels open at negative membrane potentials. *J. Gen. Physiol.* **92:**27–54

Rousseau, E. 1989. Single chloride-selective channel from cardiac sarcoplasmic reticulum studied in planar lipid bilayers. *J. Membrane Biol.* **110:**39–47

Rousseau, E., Roberson, M., Meissner, G. 1988. Properties of single chloride selective channel from sarcoplasmic reticulum. *Eur. Biophys. J.* **16:**143–151

Selwyn, M.J., Ng, L.T., Choo, H.L. 1993. The pH-dependent anion-conducting channel of the mitochondrial inner membrane is potently inhibited by zinc ions. *FEBS Lett.* **331:**129–133

Sherry, A.M., Cuppoletti, J., Malinowska, D.H. 1994. Differential acidic pH sensitivity of Delta508 CFTR Cl^- channel activity in lipid bilayers. *Am. J. Physiol. Cell Physiol.* **266:**C870–C875

Sigworth, F.J., Sine, S.M. 1987. Data transformations for improved display and fitting of single-channel dwell time histograms. *Biophys. J.* **52:**1047–1054

Smart, T.G., Constanti, A.A. 1982. A novel effect of zinc on the lobster muscle GABA receptor. *Proc. R. Soc. London* **215:**327–341

Smith, J.S., Coronado, R., Meissner, G. 1986. Single-channel calcium and barium currents of large and small conductance from sarcoplasmic reticulum. *Biophys. J.* **50:**921–928

Soejima, M., Kokubun, S. 1988. Single anion-selective channel and its ion selectivity in the vascular smooth muscle cell. *Pfluegers Arch.* **411:**304–311

Tanifuji, M., Sokabe, M., Kasai, M. 1987. An anion channel of sarcoplasmic reticulum incorporated into planar lipid bilayers: single-channel behavior and conductance properties. *J. Membrane Biol.* **99:**103–111

Townsend, C., Rosenberg, R.L. 1994. Voltage-sensitive chloride channels reconstituted from cardiac sarcolemma in planar lipid bilayers. *Biophys. J.* **66:**A420. *(Abstr.)*

Waldo, G.L., Boyer, J.L., Morris, A.J., Harden, T.K. 1991. Purification of an AlF_4^- and G-protein $\beta\gamma$-subunit-regulated phospholipase C-activating protein. *J. Biol. Chem.* **266:**14217–14225

White, M.M., Aylwin, M. 1990. Niflumic and flufenamic acids are potent reversible blockers of Ca-activated Cl channels in Xenopus oocytes. *Mol. Pharmacol.* **37:**720–724

Wilk Blaszczak, M.A., French, A.S., Man, S.F. 1992. Halide permeation through 10 pS and 20 pS anion channels in human airway epithelial cells. *Biochim. Biophys. Acta.* **1104:**160–166

Woll, K.H., Leibowitz, M.D., Neumcke, B., Hille, B. 1987. A high-conductance anion channel in adult amphibian skeletal muscle. *Pfluegers Arch.* **410:**632–640

Wright, E.M., Diamond, J.M. 1977. Anion selectivity in biological systems. *Physiol. Rev.* **57:**109–156

Yano, K., Zarain-Herzberg, A. 1994. Sarcoplasmic reticulum calsequestrins: Structural and functional properties. *Mol. Cell. Biochem.* **135:**61–70

Yellen, G. 1984. Ionic permeation and blockage in Ca^{2+}-activated K^+ channels of bovine chromaffin cells. *J. Gen. Physiol.* **95:**911–939